materials

MDPI

Article

Effect of Rolling Route on Microstructure and Tensile Properties of Twin-Roll Casting AZ31 Mg Alloy Sheets

Dan Luo [1,2], Yue Pan [1], Hui-Yuan Wang [1,*], Li-Guo Zhao [1], Guo-Jun Liu [1], Yan Liu [2,*] and Qi-Chuan Jiang [1]

[1] Key Laboratory of Automobile Materials of Ministry of Education & School of Materials Science and Engineering, Nanling Campus, Jilin University, No. 5988 Renmin Street, Changchun 130025, China; danluo198709@gmail.com (D.L.); panyue0503@163.com (Y.P.); chenl11@jlu.edu.cn (L.-G.Z.); liuguojun@jlu.edu.cn (G.-J.L.); jqc@jlu.edu.cn (Q.-C.J.)

[2] Key Laboratory of Bionic Engineering (Ministry of Education), Jilin University, Changchun 130025, China

* Correspondence: wanghuiyuan@jlu.edu.cn (H.-Y.W.); lyyw@jlu.edu.cn (Y.L.); Tel./Fax: +86-431-8509-4699 (H.-Y.W.); +86-431-8509-5575 (Y.L.)

Academic Editor: Richard Thackray
Received: 6 April 2016; Accepted: 24 May 2016; Published: 1 June 2016

Abstract: Twin-roll casting AZ31 Mg alloy sheets have been fabricated by normal unidirectional-rolling, head-to-tail rolling, and clock-rolling, respectively. It has been demonstrated that head-to-tail rolling is the most effective to refine the microstructure and weaken the basal texture among the three rolling routes. Excellent integrated tensile properties can be obtained by the head-to-tail rolling. The yield strength, ultimate tensile strength, and plastic elongation are 196 MPa, 301 MPa, and 28.9%, respectively. The strength can benefit from the fine grains (average value of 4.0 μm) of the AZ31 alloy processed by the head-to-tail rolling route, while the excellent plastic elongation is achieved owing to the weakened basal texture besides the fine grains. Results obtained here can be used as a basis for further study of some simple rolling methods, which is critical to the development of Mg alloys with high strength and plasticity.

Keywords: magnesium alloy; texture; rolling route; mechanical properties

1. Introduction

Twin-roll casting is an effective method to produce metal alloys while significantly reducing costs [1–3]. However, centerline segregation and coarse columnar dendritic grains form during the twin-roll casting process, which has a deleterious effect on the strength and ductility due to the limited quality in Mg alloys [3]. Sequential warm rolling has been developed to refine grains of Mg alloys after the twin-roll casting process [4,5]. However, such a method often results in a strong basal texture [4]. The basal texture with most grains in hard orientation is difficult to deform since the resolved shear stress in the basal plane is essentially zero, which leads to stress localization and premature failure [6,7]. Therefore, it is of significant interest to find methods to avoid the development of the basal texture during the rolling deformation process [6].

There are many reports on the weakening of the basal texture intensity and the inclining of the basal pole obtained by different methods [8–10]. Changing the rolling route has been considered to be one of the effective methods to decrease the basal texture strength and enhance the rollability of Mg alloys [11]. Higher strength and elongation can be achieved due to finer grains and weaker basal texture obtained by changing the rolling routes [12]. However, twin-roll casting is still difficult at present, and the related research about different rolling routes of cast-rolling AZ31 Mg alloy sheets have not been investigated thoroughly [6]. In this work, twin-roll casting AZ31 Mg alloy sheets have been

manufactured by normal unidirectional-rolling, head-to-tail rolling, and clock-rolling, respectively. The work focuses primarily on the microstructure and tensile properties of the hot-rolled AZ31 alloy sheets, and particular attention was paid to investigate the evolution of texture.

2. Experimental Details

The as-received AZ31 Mg alloy sheets with a thickness of 6 mm were fabricated by the twin-roll casting method. The twin-roll casting sheets were cut into rectangular slabs of 40 mm (rolling direction, RD) × 40 mm (transverse direction, TD) × 6 mm (normal direction, ND) and then were homogenized at 430 °C for 3 h before rolling. Afterwards, the slabs were hot-rolled from 6 to 1 mm after eight passes with reduction ratios of ~28%, ~24%, ~22%, ~19%, ~27%, ~9%, ~14% and ~15% successively. The slabs were preheated at 200 °C for 15 min before the first pass and for 10 min before subsequent passes. Finally, the as-rolled samples were annealed at 200 °C for 30 min.

Microstructures were observed by an optical microscope (OM) (Carl Zeiss-Axio Imager A2m, Oberkochen, Germany). The electron backscatter diffraction (EBSD) measurements were performed on a scanning electron microscope (SEM) (Zeiss Supra55 (VP), Oberkochen, Germany) with the software Channel 5. The EBSD was performed at 15 kV, with a tilt angle of 70° and a scan step of 0.6 or 4 μm. The X-ray diffraction (XRD) (D/Max 2500PC, Rigaku, Japan) was employed to analyze the phases using Cu K_α radiation in step mode from 20° to 80° with a scanning speed of 4° min^{-1} and an acquisition step of 0.02° (2θ). Samples for OM microstructure observation were firstly ground with 2000 mesh SiC papers, followed by buffing with 0.5 μm diamond pastes, and then chemically etched in acetic picral solution (5 mL acetic acid, 5 g picric acid, 10 mL distilled water, and 80 mL ethanol) for 15 s. Samples for the EBSD microstructure observation were firstly mechanically polished and then followed with argon ion polishing (Gatan Ilion II 697, Pleasanton, CA, USA) at a voltage of 8.0 kV for 15 min, 4 kV for 15 min, and 1 kV for 30 min successively. Tensile samples machined from the as-annealed sheets (a gage size of 30 mm × 10 mm × 0.7 mm) were tested along the RD on a material testing machine (INSTRON 5869, Cambridge, MA, USA) at a strain rate of 1.0×10^{-3} s^{-1}. Stress–strain curves with good repeatability have been used.

3. Results and Discussion

The optical microstructure of the homogenized twin-roll casting AZ31 alloy is shown in Figure 1a. It can be seen the grains are coarse and the grain size primarily ranges between 20 and 80 μm (the inset in Figure 1a), and the average grain size is 53 μm. To examine the orientation of the grains, EBSD measurements were performed. It can be seen that the orientation of the grains is random in the inverse pole figure (IPF) map, which indicates the basal texture is weak in the homogenized AZ31 alloy (Figure 1b). The XRD pattern further confirms that the basal texture is very weak in the homogenized AZ31 alloy (Figure 1c). Only α-Mg phase is detected by XRD (Figure 1c), which indicates that eutectic $Mg_{17}Al_{12}$ phases are thoroughly solid-dissolved after the homogenization treatment.

Figure 2 shows the schematic diagram of the three rolling routes. Route A is unidirectional-rolling, where the rolling direction is always constant (Figure 2a). Route B (head-to-tail rolling), differing from the normal unidirectional rolling, has two rolling directions (Figure 2b). The rolling direction of Route B is changed by 180° repeatedly (Figure 2b). The last one is Route C (clock-rolling), where the rolling direction is changed anticlockwise by 90° after each rolling (Figure 2c).

Optical microstructures of the as-annealed AZ31 alloy processed by Route A, B, and C are presented, respectively in Figure 3a–c. It can be observed that the microstructure of as-annealed samples is completely recrystallized. Fine and equiaxed grains form by the three rolling methods. The average grain sizes are 4.4, 4.0, and 7.3 μm, respectively (Figure 3a–c). Compared with the microstructure of the AZ31 alloy processed by Route A, the one processed by Route B is refined, which is similar to the result of the AZ31 Mg alloy sheets rolled by changing the rolling route (cross-rolling, rotating the specimen by 90° after each rolling step back and forth) in previous research [12]. It has been reported that the grains of the AZ31 alloy processed by cross-rolling are finer than those processed

by the unidirectional-rolling (Route A). The strain path can define the microstructure of a sample during the rolling deformation process, and grains usually tend to be elongated towards the rolling direction after each rolling [6]. Dynamic recovery (DRV) can be promoted by the constant change of the microstructure, which in turn influences the behavior of the recrystallization [6]. However, the microstructure processed by Route C consists of more coarse grains compared with the ones processed by Route A and B (Figure 3c), which causes an adverse effect on the grain size of the AZ31 alloy, probably due to relatively weak shear deformation between each rolling pass.

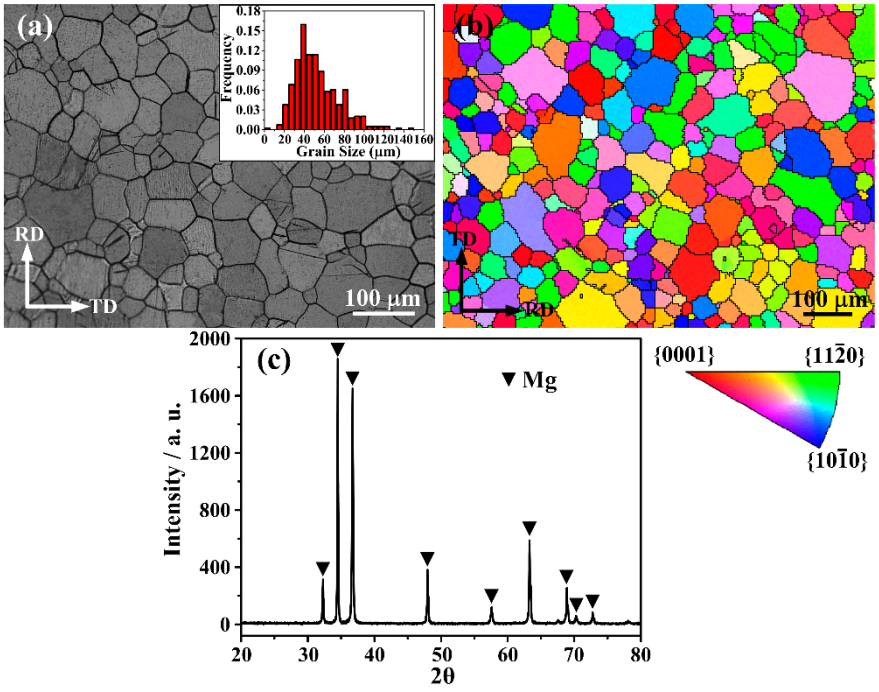

Figure 1. (**a**) Optical micrograph with the top-right corner inset showing a grain size distribution; (**b**) inverse pole figure (IPF) map and (**c**) X-ray diffraction (XRD) pattern of the homogenized AZ31 Mg alloy at 430 °C for 3 h.

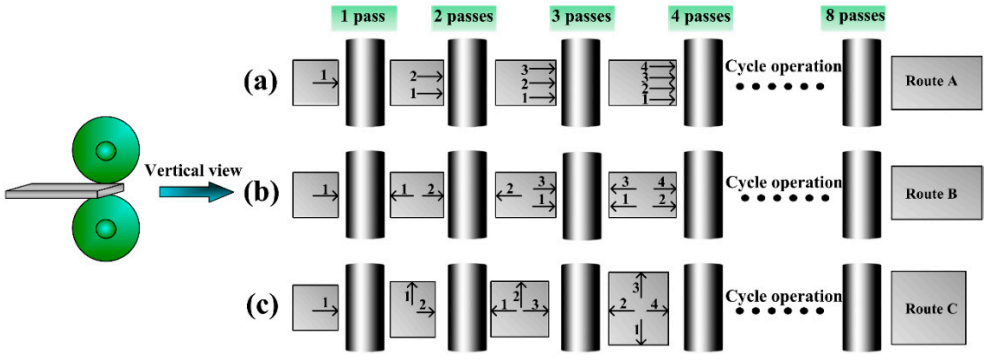

Figure 2. Schematic diagrams of the three rolling methods: (**a**) Route A; (**b**) Route B; and (**c**) Route C.

To examine the microstructure in detail, IPF maps of the as-annealed AZ31 Mg alloy sheets processed by Route A, B, and C are shown in Figure 4. Color difference of the homogenized AZ31 alloy shows that the orientation of the c-axis of the grains is random (Figure 1b), while the three rolling methods give rise to the rotation of c-axis, and the c-axis of most of the grains are parallel to the normal direction due to the increasingly accumulated strain (Figure 4). Note that grains are refined in the

microstructure processed by Route B (Figure 4b), which is consistent with the result from the optical microstructure (Figure 3b).

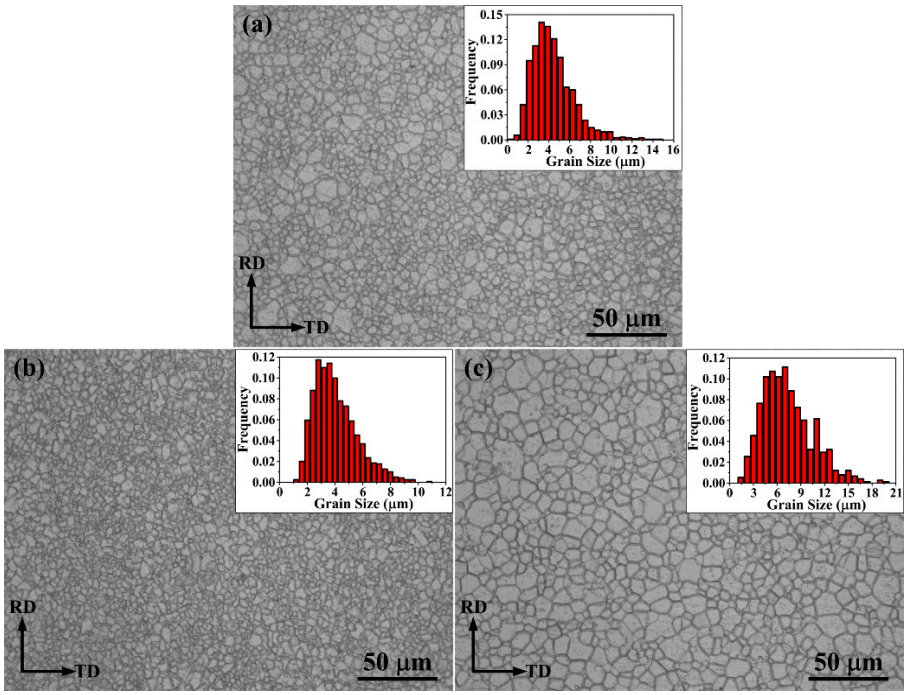

Figure 3. Optical micrographs with the top-right corner insets showing the grain size distribution of the as-annealed AZ31 Mg alloy processed by (**a**) Route A; (**b**) Route B; and (**c**) Route C, respectively.

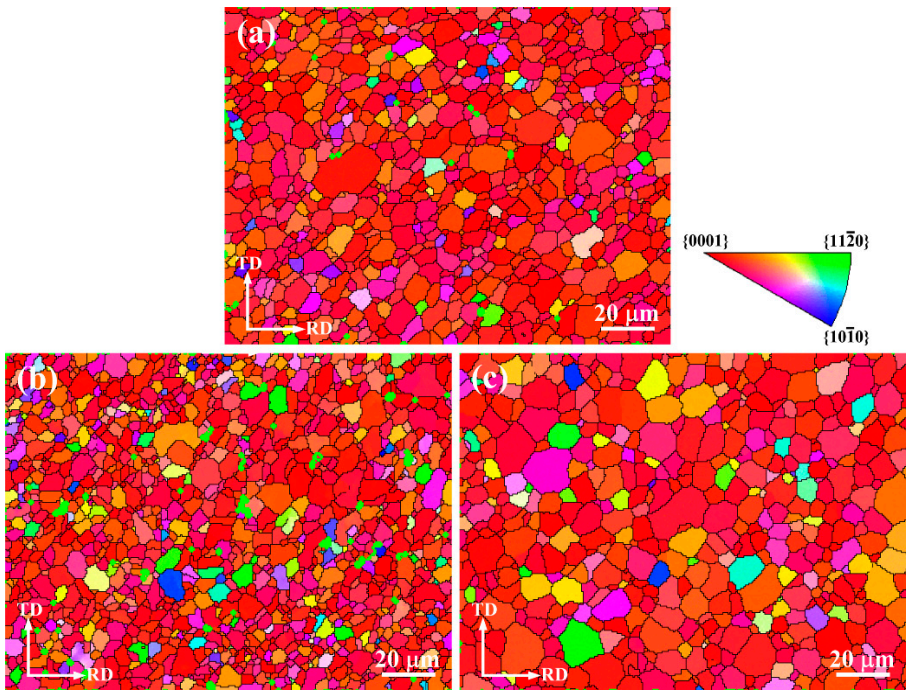

Figure 4. IPF maps of the as-annealed AZ31 Mg alloy processed by (**a**) Route A; (**b**) Route B; and (**c**) Route C, respectively.

Figure 5 shows the (0002) pole figures of the AZ31 alloy before and after the rolling by different routes. In the initial homogenized AZ31 alloy, the basal texture intensity is 4.7 and it can be seen that disperse texture components form in Figure 5a, which shows that the texture is weak and is consistent with the result from the IPF microstructure in Figure 1b. The basal texture intensity is 15.1, 13.4, and 14.4 for the AZ31 alloy sheets processed by Route A, B, and C, respectively. The AZ31 alloy sheet processed by Route A shows a typical strong basal texture (Figure 5b), where the distribution of the orientation around the normal direction is wider in the rolling direction compared with the one in the transverse direction [12]. The formation of strong basal texture in rolled AZ31 can be attributed to both of the basal <**a**> slip and tensile twinning [13–15]. The AZ31 alloy sheet processed by Route B also exhibits typical basal texture, but the texture has been weakened by the constant change of rolling direction in Figure 5c. The AZ31 alloy sheet processed by Route C shows stronger texture than the one processed by Route B, but the texture is still weaker than the one processed by Route A. Therefore, the basal texture can be weakened by both the head-to-tail rolling and clock-rolling. Moreover, note that basal pole tends to split in the Figure 5d. It has been reported that pyramidal <**c** + **a**> slip is responsible for the split of the basal pole [14,15]. The critical resolved shear stresses (CRSSs) of non-basal slips (such as the pyramidal <**c** + **a**> slip) decrease substantially with the increase of the temperature [16]. The CRSS of the pyramidal slip at room temperature is about 100 times larger than that of the basal slip [17]. This value decreases as the temperature rises, which means that the non-basal slip is much easier activated at elevated temperatures [18,19]. As such, it can be deduced that the AZ31 alloy sheet processed by Route C at 200 °C exhibits a tendency of splitting probably on account of the activation of the non-basal slips here.

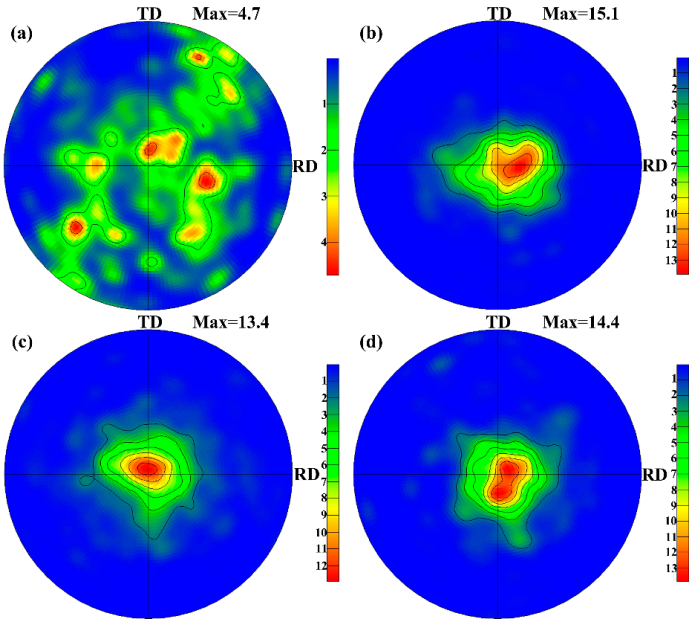

Figure 5. (0 0 0 2) pole figures of the AZ31 Mg alloy before and after the rolling by different routes: (**a**) homogenized; (**b**) Route A; (**c**) Route B; and (**d**) Route C, respectively.

Tensile engineering stress–strain curves of the as-annealed AZ31 alloy sheets processed by the three methods are plotted in Figure 6. Average tensile properties are presented in Table 1, which includes the yield strength ($\sigma_{0.2}$), ultimate tensile strength (σ_b), elongation-to-failure (δ_f), and plastic elongation (δ_P). The $\sigma_{0.2}$ and σ_b for Route A and B are nearly identical with actual errors. Note that the δ_f and δ_P obviously increase from 26.7% and 23.3% to 30.9% and 28.9%, respectively. However, the mechanical properties of the AZ31 alloy processed by Route C decreases compared with the ones of Route B. Therefore, the AZ31 alloy sheet processed by Route B presents excellent integrated mechanical

properties among the three rolling routes. Table 2 shows tensile properties of some rolling AZ31 alloy in literatures [14,20–28]. It can be found that the AZ31 alloy sheet processed by Route B also shows excellent integrated tensile properties compared with the reported rolling AZ31 alloys.

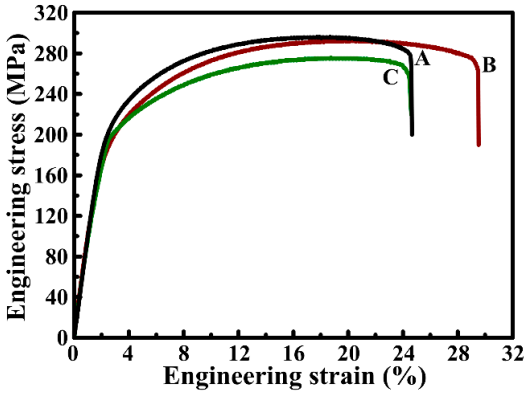

Figure 6. Tensile engineering stress–strain curves AZ31 Mg alloy sheets processed by (**A**) Route A; (**B**) Route B; and (**C**) Route C, respectively.

Table 1. Tensile properties of the as-annealed AZ31 alloy sheets processed by the three rolling methods at room temperature.

Route	$\sigma_{0.2}$/MPa	σ_b/MPa	δ_f/%	δ_P/%
A	199^{+5}_{-8}	298^{+2}_{-2}	$26.7^{+2.7}_{-2.1}$	$23.3^{+2.3}_{-1.3}$
B	196^{+1}_{-1}	301^{+13}_{-9}	$30.9^{+0.7}_{-1.3}$	$28.9^{+0.7}_{-1.1}$
C	192^{+8}_{-7}	280^{+4}_{-5}	$25.8^{+1.2}_{-1.2}$	$24.0^{+0.8}_{-1.4}$

Table 2. Tensile properties of rolling AZ31 alloy in the literature.

Alloy	Grain Size (μm)	$\sigma_{0.2}$/MPa	σ_b/MPa	δ_f/%	δ_P/%
AZ31 [14]	10.2	161	272	19.7	~
AZ31 [24]	10	~	273	~	8
AZ31 [25]	~	250	295	~	16.2
AZ31B [26]	7.2	167	263	25.8	
AZ31 [27]	~	254	320	~	13.0
AZ31 [28]	~	180	270	19%	~
AZ31 [29]	7.4	158	280	20.3	~
AZ31 [30]	13	147	306	27.3	~
AZ31 [31]	3~20	175	277	~	21
AZ31 [32]	2.8	290	~310	~	23

The strength of the AZ31 alloy processed by both Route A and B are nearly identical, although the texture of Route A alloy has been weakened. Therefore, it can be deduced that the strength of the Route B alloy benefits from the finer grain size compared with the Route A alloy. It should also be noted that the δ_P is observably improved by Route B. In general, conventional rolled Mg sheets present a typical basal texture where most basal poles are parallel to the sheet plane [20–22]. In this case (RD tension), strain localization and premature shear failure occur on account of the suppression of the basal slip with the Schmid factor (SF) of zero [6,23]. Therefore, the excellent δ_P can be attributed to the weakened basal texture besides the fine grains in the AZ31 alloy produced by Route B. Conversely, the mechanical properties of the AZ31 alloy rolled by Route C decrease compared with the ones rolled by Route B, which can be caused by coarse grains in the alloy (Figure 3c). Therefore, excellent mechanical properties can be obtained by Route B due to the fine grains with weakened basal texture.

4. Conclusions

In the present study, the effects of three rolling routes on the microstructure and tensile properties of twin-roll casting AZ31 Mg alloy sheets were investigated. The grain size of the as-annealed AZ31 alloy processed by Route A (unidirectional-rolling), B (head-to-tail rolling), and C (clock-rolling) is 4.4, 4.0, and 7.3 μm, respectively. The basal texture intensity is 15.1, 13.4, and 14.4 for the Route A, B, and C, respectively. Route B is the most effective at refining the microstructure and weakening the basal texture among the three rolling routes. The AZ31 alloy sheet processed by Route B presents excellent integrated tensile properties. The corresponding $\sigma_{0.2}$, σ_b, δ_f, and δ_P are 196 MPa, 301 MPa, 30.9%, and 28.9%, respectively. The tensile strength can benefit from the fine grains of the AZ31 alloy processed by the head-to-tail rolling route, while the excellent plastic elongation is achieved owing to the weakened basal texture besides the fine grains.

Acknowledgments: Financial support from The Natural Science Foundation of China (Nos. 51271086 and 51301074) and The Research Project of Science and Technology of the Department of Education of Jilin Province (2015-482) are greatly acknowledged. Partial financial support came from The Fundamental Research Funds for Jilin University (JCKY-QKJC02), China Postdoctoral Science Foundation (2016M590262), and The ChangBai Mountain Scholars Program (2013014).

Author Contributions: Dan Luo, Hui-Yuan Wang, Guo-Jun Liu, Yan Liu and Qi-Chuan Jiang conceived and designed the experiments; Li-Guo Zhao, Dan Luo and Yue Pan performed the experiments; Dan Luo and Hui-Yuan Wang analyzed the data; Dan Luo wrote the paper. All authors reviewed the manuscript.

Conflicts of Interest: The authors declare no conflict of interest.

References

1. Geng, J.; Nie, J.F. Unloading yield effect in a twin-roll-cast Mg–3Al–1Zn alloy. *Scr. Mater.* **2015**, *100*, 78–81. [CrossRef]
2. Málek, P.; Poková, M.Š.; Cieslar, M. High Temperature Deformation of Twin-Roll Cast Al-Mn-Based Alloys after Equal Channel Angular Pressing. *Materials* **2015**, *8*, 7650–7662. [CrossRef]
3. Das, S.; Barekar, N.; Fakir, O.E.; Yang, X.; Dear, J.P.; Fan, Z. Influence of intensive melt shearing on subsequent hot rolling and the mechanical properties of twin roll cast AZ31 strips. *Mater. Lett.* **2015**, *144*, 54–57. [CrossRef]
4. Kim, K.H.; Suh, B.C.; Bae, J.H.; Shim, M.S.; Kim, S.; Kim, N.J. Microstructure and texture evolution of Mg alloys during twin-roll casting and subsequent hot rolling. *Scr. Mater.* **2010**, *63*, 716–720. [CrossRef]
5. Chen, H.M.; Zang, Q.H.; Yu, H.; Zhang, J.; Jin, Y.X. Effect of intermediate annealing on the microstructure and mechanical property of ZK60 magnesium alloy produced by twin roll casting and hot rolling. *Mater. Charact.* **2015**, *106*, 437–441. [CrossRef]
6. Al-Samman, T.; Gottstein, G. Influence of strain path change on the rolling behavior of twin roll cast magnesium alloy. *Scr. Mater.* **2008**, *59*, 760–763. [CrossRef]
7. Cepeda-Jiménez, C.M.; Pérez-Prado, M.T. Microplasticity-Based rationalization of the room temperature yield asymmetry in conventional polycrystalline Mg alloys. *Acta Mater.* **2016**, *108*, 304–316. [CrossRef]
8. Sarebanzadeh, M.; Roumina, R.; Mahmudi, R.; Wu, G.H.; Jafari Nodooshan, H.R. Enhancement of superplasticity in a fine-grained Mg–3Gd–1Zn alloy processed by equal-channel angular pressing. *Mater. Sci. Eng. A* **2015**, *646*, 249–253. [CrossRef]
9. Seipp, S.; Wagner, M.F.X.; Hockauf, K.; Schneider, I.; Meyer, L.W.; Hockauf, M. Microstructure, crystallographic texture and mechanical properties of the magnesium alloy AZ31B after different routes of thermo-mechanical processing. *Int. J. Plasticity* **2012**, *35*, 155–166. [CrossRef]
10. Zhang, X.H.; Cheng, Y.S. Tensile anisotropy of AZ91 magnesium alloy by equal channel angular processing. *J. Alloys Compd.* **2015**, *622*, 1105–1109. [CrossRef]
11. Hu, Z.; Chen, Z.Y.; Xiong, J.Y.; Chen, T.; Shao, J.B.; Liu, C.M. Microstructure and mechanical properties of Mg–6.75%Zn–0.57%Zr–0.4%Y–0.18%Gd sheets by unidirectional and cross rolling. *Mater. Sci. Eng. A* **2016**, *662*, 519–527. [CrossRef]

12. Zhang, H.; Huang, G.S.; Roven, H.J.; Wang, L.F.; Pan, F.S. Influence of different rolling routes on the microstructure evolution and properties of AZ31 magnesium alloy sheets. *Mater. Des.* **2013**, *50*, 667–673. [CrossRef]
13. Styczynski, A.; Hartig, Ch.; Bohlen, J.; Letzig, D. Cold rolling textures in AZ31 wrought magnesium alloy. *Scr. Mater.* **2004**, *50*, 943–947. [CrossRef]
14. Zhou, T.; Yang, Z.; Hu, D.; Feng, T.; Yang, M.B.; Zhai, X.B. Effect of the final rolling speeds on the stretch formability of AZ31 alloy sheet rolled at a high temperature. *J. Alloys Compd.* **2015**, *650*, 436–443. [CrossRef]
15. Yan, H.; Chen, R.S.; Han, E.H. Room-Temperature ductility and anisotropy of two rolled Mg–Zn–Gd alloys. *Mater. Sci. Eng. A* **2010**, *527*, 3317–3322. [CrossRef]
16. Chapuis, A.; Driver, J.H. Temperature dependency of slip and twinning in plane strain compressed magnesium single crystals. *Acta Mater.* **2011**, *59*, 1986–1994. [CrossRef]
17. Yoo, M.H. Slip, Twinning, and Fracture in Hexagonal Close-Packed Metals. *Metall. Trans. A* **1981**, *12A*, 409–418. [CrossRef]
18. Máthis, K.; Nyilas, K.; Axt, A.; Dragomir-Cernatescu, I.; Ungár, T.; Lukáč, P. The evolution of non-basal dislocations as a function of deformation temperature in pure magnesium determined by X-ray diffraction. *Acta Mater.* **2004**, *52*, 2889–2894. [CrossRef]
19. Jëger, A.; Lukáč, P.; Gärtnerová, V.; Bohlen, J.; Kainer, K.U. Tensile properties of hot rolled AZ31 Mg alloy sheets at elevated temperatures. *J. Alloys Compd.* **2004**, *378*, 184–187. [CrossRef]
20. Zeng, Z.R.; Bian, M.Z.; Xu, S.W.; Davies, C.H.J.; Birbilis, N.; Nie, J.F. Texture evolution during cold rolling of dilute Mg alloys. *Scr. Mater.* **2015**, *108*, 6–10. [CrossRef]
21. Yi, S.B.; Bohlen, J.; Heinemann, F.; Letzig, D. Mechanical anisotropy and deep drawing behaviour of AZ31 and ZE10 magnesium alloy sheets. *Acta Mater.* **2010**, *58*, 592–605. [CrossRef]
22. Agnew, S.R.; Nie, J.F. Preface to the viewpoint set on: The current state of magnesium alloy science and technology. *Scr. Mater.* **2010**, *63*, 671–673. [CrossRef]
23. Li, X.; Al-Samman, T.; Gottstein, G. Mechanical properties and anisotropy of ME20 magnesium sheet produced by unidirectional and cross rolling. *Mater. Des.* **2011**, *32*, 4385–4393. [CrossRef]
24. Hua, X.; Lv, F.; Wang, Q.; Duan, Q.Q.; Zhang, Z.F. Achieving synchronous improvement of strength and ductility of Mg–3%Al–1%Zn alloy through controlling the rolling orientation. *Mater. Sci. Eng. A* **2013**, *586*, 38–44. [CrossRef]
25. Guo, F.; Zhang, D.F.; Yang, X.S.; Jiang, L.Y.; Pan, F.S. Influence of rolling speed on microstructure and mechanical properties of AZ31 Mg alloy rolled by large strain hot rolling. *Mater. Sci. Eng. A* **2014**, *607*, 383–389. [CrossRef]
26. Huang, X.S.; Chino, Y.; Mabuchi, M.; Matsuda, M. Influences of grain size on mechanical properties and cold formability of Mg–3Al–1Zn alloy sheets with similar weak initial textures. *Mater. Sci. Eng. A* **2014**, *611*, 152–161. [CrossRef]
27. Guo, F.; Zhang, D.F.; Yang, X.S.; Jiang, L.Y.; Chai, S.S.; Pan, F.S. Effect of rolling speed on microstructure and mechanical properties of AZ31 Mg alloys rolled with a wide thickness reduction range. *Mater. Sci. Eng. A* **2014**, *619*, 66–72. [CrossRef]
28. Ma, R.; Wang, L.; Wang, Y.N.; Zhou, D.Z. Microstructure and mechanical properties of the AZ31 magnesium alloy sheets processed by asymmetric reduction rolling. *Mater. Sci. Eng. A* **2015**, *638*, 190–196. [CrossRef]
29. Zhang, H.; Cheng, W.L.; Fan, J.F.; Xu, B.S.; Dong, H.B. Improved mechanical properties of AZ31 magnesium alloy sheets by repeated cold rolling and annealing using a small pass reduction. *Mater. Sci. Eng. A* **2015**, *637*, 243–250. [CrossRef]
30. Zhang, H.; Huang, G.S.; Wang, L.F.; Roven, H.J.; Pan, F.S. Enhanced mechanical properties of AZ31 magnesium alloy sheets processed by three-directional rolling. *J. Alloys Compd.* **2013**, *575*, 408–413. [CrossRef]
31. Zúberová, Z.; Kunz, L.; Lamark, T.T.; Estrin, Y.; Janeček, M. Fatigue and Tensile Behavior of Cast, Hot-Rolled, and Severely Plastically Deformed AZ31 Magnesium Alloy. *Metall. Mater. Trans. A* **2007**, *38A*, 1934–1940. [CrossRef]
32. Miao, Q.; Hu, L.N.; Wang, G.J.; Wang, E.D. Fabrication of excellent mechanical properties AZ31 magnesium alloy sheets by conventional rolling and subsequent annealing. *Mater. Sci. Eng. A* **2011**, *528*, 6694–6701. [CrossRef]